# EFFECTS OF BLOWING RATIO ON THE HEAT TRANSFER COEFFICIENT DISTRIBUTION DOWNSTREAM OF A SINGLE FILM COOLING HOLE

A.R Abu Talib[1], A.A Jaafar[1], A.S Mokhtar[1], Mohd Saiah H.R[1], I. Abd. Rahim[2] and M.S Abdul Karim[3]
[1]Department of Aerospace Engineering, Universiti Putra Malaysia, 43400 Selangor, Malaysia.
[2]School of Manufacturing Engineering, Kolej Universiti Kejuruteraan Utara Malaysia, 01000 Perlis, Malaysia
[3]Dept. of Manufacturing Design, Kolej Universiti Teknikal Kebangsaan Malaysia, 75450, Melaka, Malaysia
Email: abrahim@eng.upm.edu.my

## *ABSTRACT*

*Detailed distributions of heat transfer coefficients downstream of a single film cooling hole were presented. The film cooling hole has an angle of inclination of 45° and a circular shape diameter of 10 mm. Tests were conducted in a purpose built heat transfer rig at the Department of Aerospace Engineering, UPM. The rig has been modified to conduct transient heat transfer testing using thermochromic liquid crystal technique. A single narrow-band liquid crystal was used to map the distribution of heat transfer coefficient downstream of a single film cooling hole at a blowing ratio ranging between 0.5-0.94. The detailed heat transfer coefficient distributions provide a clear understanding of free jet-mainstream interactions for different blowing ratio. Results shows that blowing ratio of 0.64 provides a better cooling protection compared to the other blowing ratios tested.*

***Keywords:*** *heat transfer coefficient, film cooling, thermochromic liquid crystal, blowing ratio.*

## INTRODUCTION

New techniques and materials are still being developed by researchers to find ways to allow a turbine engine to operate under high temperature environment. Film cooling technique is one of the effective techniques available these days used in order to cool the turbine blades to be able to operate in high temperature environment. There are several applicable cooling methods that have been introduced over the years. These cooling methods are such as air cooling, water cooling, steam cooling, and fuel cooling. Air cooling method is common among large aerospace turbine engines. The air used for the cooling method is usually bled from various parts in the compressor stage. There are two categories of air cooling method which are: (a) Internal cooling - The hot mainstream temperature ranging from 1300°K to 1600°K. This category includes convective cooling, impingement cooling and internally air cooled thermal barrier, and (b) External Cooling - The external stream temperature ranging more than 1600°K. This type of category includes local film cooling, full coverage film cooling and transpiration cooling.

In film cooling technique, the coolant air will be ejected through the cooling holes covering the turbine blade. The ejected cool air will act as a buffer between the turbine blade and the high temperature environment. There are several factors that would affect the efficiency of the cooling process by this film cooling technique such as the diameter, shape, inclination, compound angle, position of the film cooling holes, turbulence intensity of the mainstream flow, the Reynolds number, and the blowing ratio.

### Film Cooling Hole Modifications

Earlier studies in film cooling technique were mostly considering injection from a single row of discrete holes. Due to the three-dimensional character of flow field downstream of the coolant injection, the cooling effectiveness decreases compared to injection from a continuous slot. In order to improve the lateral distribution of the injected coolant and to approach a two-dimensional film cooling situation, more studies were focused on the injection from a double row of cylindrical holes in staggered arrangement and also using a single row of fan-shaped holes. Fan-shaped holes present very good effectiveness values especially close behind the injection. Due to lateral expansion of hole, the injected coolant is evenly spread which results in a quite uniform surface temperature distribution. As the injection velocity increases, the film cooling effectiveness also increases. In the case of double row of cylindrical holes in staggered arrangement, good performance was found in low and medium injection velocity. Due to staggered arrangement, the coolant is well spread in the lateral direction and

quite uniform distribution of effectiveness is achieved. At high injection velocity, M>1, the cooling jets starts to separate from the wall which is more pronounced for the first row due to the blockage effect of the second row [1].

There are only a few studies in the literature that dealt with large stream-wise angle. Nasir et al. [2] studied the effect of compound angle injection on flat surface film cooling with large steam-wise angle. Film cooling measurements are presented over a flat surface through a single row of discrete holes angled 55° along the stream-wise direction. The holes are angled 0° and 60° in the lateral direction to study the effect of compound angle injection. Tests were conducted in a low speed wind tunnel with the Reynolds number of 9500 and free-stream velocity is set at 11%. The usage of thermochromic liquid crystal (TLC) measurement technique was used to measure both local heat transfer coefficient and film effectiveness results simultaneously. Film cooling effectiveness is generally lower for a large stream wise angle of 55° compared to the typically used shallow angle of 35°. The compound angle of 60° provides significantly higher film cooling effectiveness than the simple injection case but also causes much higher heat transfer coefficients. Overall, the compound angle injection with large stream wise angle holes provide improved performance compared to simple angle injection geometry.

Investigation on the effect of various stream-wise angles was conducted by Yuen and Martinez-Botaz [3-4]. Film cooling effectiveness were studied experimentally on a cylindrically hole with a stream-wise angle of 30°, 60° and 90°, in a flat plate test facility with zero pressure gradient. The blowing ratio ranges from 0.33 to 2, and the free-stream Reynolds number was 8563. The results were, maximum effectiveness was achieved by the 30° hole in the immediate region with a blowing ratio of 0.33 that was approximately 20% higher than that by the steeper (60° and 90°) holes. They also found that film cooling at high blowing ratios was not as effective as at low blowing ratios.

## Flow Characteristics

The literature on the utilization of the TLC for film cooling effectiveness and heat transfer investigations on a flat plate and a turbine airfoil were done by Drost et al. [5]. Flat plate film cooling was investigated for a single row of 35° inclined holes at Mach number 0.3 and 0.5. Downstream of the injection heat transfer was increase in between the holes due to enhanced turbulence caused by the shearing of the coolant and the mainstream. The TLC technique has been successfully used for film cooling measurements on a flat plate and a turbine airfoil. Heat transfer results were good agreement for low momentum flux ratios, but showed increase values at higher coolant momentum. Main-stream turbulence reduce flat plate effectiveness at low and moderate blowing ratios, but increases the effectiveness at high blowing ratios due to a better dispersion of the detaching jets in the boundary layer.

Mayhew et al. [6] reported that the adiabatic effectiveness on a film cooled flat plate in a low turbulence environment. Film cooling performance of a flat plate in the presence of low and high freestream turbulence is investigated using liquid crystal thermography. They contributed high resolution colour images that clearly show how the free-stream turbulence spreads the cooling air around a larger area of film cooled surface. The distributions of the adiabatic effectiveness are determined over the film cooled surface of the flat plate using the hue method and image processing. Three blowing ratios were investigated for a model with three straight holes spaced three diameters apart, with density ratio near unity. High free-stream turbulence is shown to increase the area-averaged effectiveness at high blowing rates, but decrease it at low blowing rates. At low blowing ratio, free-stream turbulence clearly reduces the coverage area of the cooling air due to increases mixing with the main flow. However, at high blowing ratio, when much of the jets has lifted off in the low turbulence case, high free-stream turbulence turns its increased mixing into an asset, entraining some of the coolant that penetrates into the main flow and mixing it with the air near the surface.

Researchers nowadays are getting more interested in film injection with compound angle orientations because this configuration provides more uniform and improved film coverage compared to that with simple angle injection [7]. The above literature was on the flow unsteadiness which is most recently recognized to have dramatic effects on film cooling. Their research was on the effect of bulk flow pulsations on film cooling with compound angle holes. A row of five film cooling holes was considered with orientation angles of 0°, 30°, 60°, and 90° at a fixed inclination angle of 35°. Static pressure pulsations are produced by an array of six rotating shutter blades, which extend across the span of the exit of the wind tunnel section. The pulsation frequency is fixed at 36 Hz, but changes in the time-average blowing ratios of 0.5, 1.0 and 2.0. Detailed film cooled boundary layer temperature distributions were measured by a cold wire and the adiabatic film cooling effectiveness by TLC. The boundary layer temperature surveys showed that pulsations induce large disruptions

to the boundary layer temperature distribution and the film coverage. As the orientation angle increases, the injectant concentration spreads further into the span-wise direction because of pulsations than the steady case. With pulsations, the adiabatic film cooling effectiveness value decreases regardless of the orientation angle. The amount of reduction however, depends on the orientation angle in such a way that the larger the orientation angle is, the smaller the reduction is.

Mostly literatures on film cooling technique use flat plate as their test section. One of the literature that use the turbine blade as their test section was by Garg and Gaugler [8]. They reported the effect of coolant temperature and mass flow on film cooling of turbine blades. A three dimensional Navier-Stokes code has been used to study the effect of coolant temperature and coolant to main-stream mass flow ratio on the adiabatic effectiveness of a film cooled turbine blade. The blade chosen was the VKI rotor with six rows of cooling holes including three rows on the shower head. The main-stream is akin to that under real engine conditions with stagnation temperature 1900K and stagnation pressure 3 MPa. Generally, the adiabatic effectiveness is lower for a higher coolant temperature due to nonlinear effect via the compressibility of air. However, over the suction side of the shower-head holes, the effectiveness is higher for a higher coolant temperature than that for a lower coolant temperature when the coolant to main-stream mass flow ratio is 5% or more. For a fixed coolant temperature, the effectiveness passes through minima on the suction side of the shower-head holes as the coolant to main-stream mass flow ratio increases. Meanwhile, on the suction side of the shower-head holes, the effectiveness decreases with increase in coolant mass flow due to coolant jet lift-off. In all cases, the adiabatic effectiveness is highly three-dimensional. They stated that studies on a flat plate could not reveal these differences.

The objective of this paper is to provide detailed measurements of heat transfer coefficient distribution downstream from a single film cooling hole for blowing ratio of 0.5, 0.64, 0.83 and 0.94 using transient liquid crystal technique.

## TEST APPARATUS AND INSTRUMENTATIONS

The test plates and some parts of the test rig were designed using Solid Works 2003 CAD application software and being fabricated using the Modella Pro CAM software MDX-650 engraving machine. The test section of an existing experimental rig reported by Jaafar et al. [9] was modified. There are two different test plates involved. Both test plates have the same geometrical dimension with their width and length is 250 mm to fit into the test section. The concerns were more onto the thickness of the test plate. 12 mm thickness plate is chosen to delay the time required for the heat applied to one surface of the test plate to penetrate through the other surface of the test plate so that the one-dimensional semi infinite solid heat transfer assumption can be used. Calibrations were done to determine the time required for the heat transferred to penetrate through the wall. As the heat transferred reached the back surface of the wall, the heat transferred will conduct laterally and the one-dimensional heat transfer assumption is no more valid.

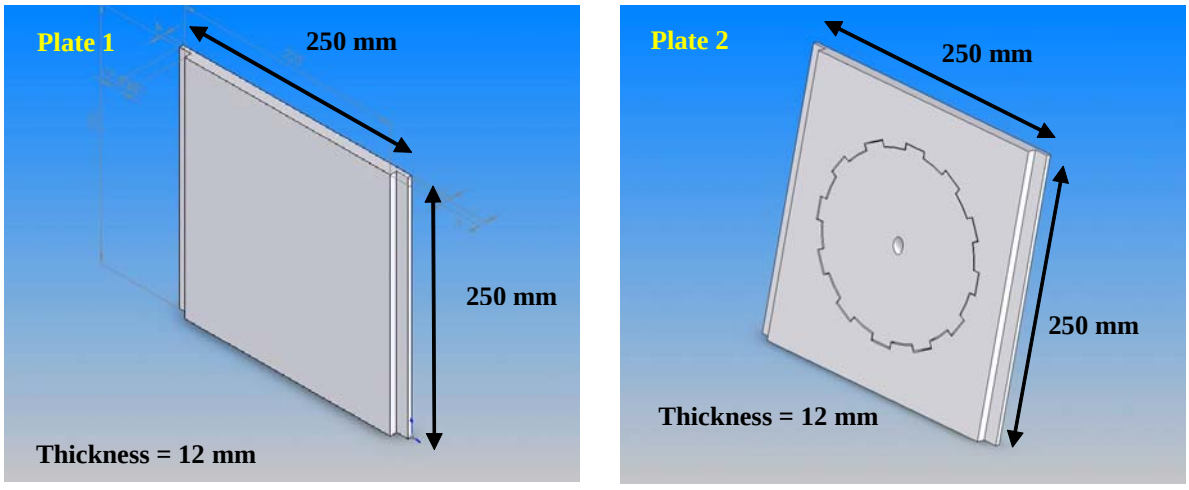


*Figure 1: Test plate 1 and 2*

Test Plate 1 (Figure 1), also regarded as a calibration plate for which the results obtained will be compared with existing correlation for the present study. The test plate 1 will be use for investigating the local heat transfer coefficient on a flat surface. The temperature distribution resulting from the heated flow will be observed at this

area. Test Plate 2 (Figure 1), will be use to investigate the effect of blowing ratio on the distribution of heat transfer coefficient distribution. There will be only one film cooling hole with the diameter of 10 mm and inclined at 45°. The inclination angle of 45° was chosen due to the limitation on the fabrication of the cooling hole as reported by Mohd Saiah [10]. The compound angle of the film cooling hole can be rotated at 0°, 30°, 60°, and 90°. However, the test only be conducted at 0° for the current study.

A Foil Thermocouple from Rhopoint, with thickness of 0.001 mm was glued to each of the test plates at 3*d* (30 mm) downstream from the centre of the plate. SpeedBonder(TM) 326 Structural Adhesive glue from Loctite was used. This type of glue was smoothly applied on the prescribed location. The glue layer must be thin so that the thin thermocouple could respond accurately to the surface temperature of the test plate. The upper surface of the test plates were sprayed using mat black paint, which provide efficient background colour plane for the TLC. The TLC will appear colourless under event temperature point and over its' clearing temperature point. Eventually those states, only the background colour was visible. Between those states, the TLC will reflect some wavelength of visible light spectrum as heat is continuously applied.

The TLC used was a narrow band sprayable TLC coating with a serial number of BM/R40C1W/C17-10 and the binder used was a sprayable Aqueous Binder coating with a serial number of ABQ-2. The TLC, binder and a little of water were mixed together by the ratio of:

| TLC | : | BINDER | : | WATER |
|---|---|---|---|---|
| 5 | : | 1 | : | 6 |

## HEAT TRANSFER TEST

One dimensional semi-infinite solid assumption was used to obtain the local heat transfer coefficient ($h$) over a surface coated with liquid crystals. The approach is similar to the approach reported by Ekkad and Han [11]. In order to apply this assumption, a low thermal conductivity and low thermal diffusivity material was used for the test plate. The one-dimensional transient conduction equation on liquid crystal coated surface were:

$$k\frac{\partial^2 T}{\partial x^2} = \rho c_p \frac{\partial T}{\partial t} \tag{1}$$

With boundary conditions:

At $t = 0, T = T_i$

At $x = 0, \quad -k\frac{\partial T}{\partial x} = h(T_w - T_m)$

At $x \to \infty, T = T_i$

Equation (1) was theoretically solved using the initial and boundary conditions, and the resulting non-dimensional temperature at the convective boundary surface (at $x = 0$) is given by:

$$\frac{T_w - T_i}{T_m - T_i} = 1 - \exp(\frac{h^2 \alpha t}{k^2}) erfc(\frac{h\sqrt{\alpha t}}{k}) \tag{2}$$

The time of colour change of the liquid crystal coating at each pixel was determined using image processing system. Equation (2) was used to calculate the heat transfer coefficient ($h$). The test conditions were set between 10 and 90 seconds. This enables the validity of the semi infinite solid assumption on the test surface, as the test duration does not allow for the heat completely penetrates across the test wall. The penetration depth calculation for the heat pulse into the substrate was reported by Schultz and Jones [12].

Film cooling technique deals with three-temperature problem involving mainstream temperature ($T_m$), coolant temperature ($T_c$), and the wall temperature ($T_w$). In film cooling situations, the mainstream temperature ($T_m$) in equation (2) was being replaced by film temperature ($T_f$), which was a mixed temperature between the mainstream and coolant temperatures that governs the convection from the liquid crystal coated surface.

The non-dimensional temperature, that was defined as film cooling effectiveness ($\eta$) was given below:

$$\eta = \frac{T_f - T_m}{T_c - T_m}$$

In which $T_f$ can be determined as

$$T_f = \eta T_c + (1-\eta) T_m \tag{3}$$

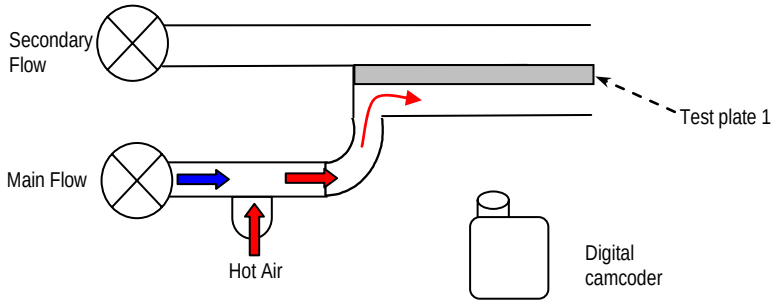


*Figure 2: Schematic diagram of the experimental setup for test 1*

Two consecutive experiments were conducted, first using the Test Plate 1, followed by Test Plate 2. For the first test, experiments were conducted only using the heated mainstream flow Figure 2. The mainstream flow was heated using two hair dryers to apply heated flow into the test section. There were four K-type thermocouples used. Two of them were used to measure the mainstream flow temperature, one of them was connected to the foil thermocouple located at the upper surface of the test plate, and the last one was placed at the back surface of the test plate to observe the back temperature of the test plate.

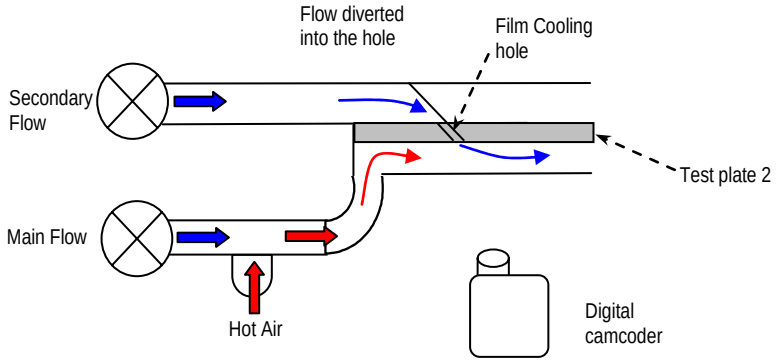


*Figure 3: Schematic diagram of the experimental setup for test 2*

The second experiment was conducted using Test Plate 2 at 0° compound angle location. This experiment was conducted with a heated mainstream flow and a secondary flow at room temperature Figure 3. The secondary flow acted as a coolant flow which was ejected through the film cooling hole. Experiments were conducted using blowing ratio ranging from 0.5-0.94. This selection of the blowing ratio was chosen due to the limitation of the experimental rig design. The equation for blowing ratio was shown below:

$$m = \frac{\rho_c v_c}{\rho v} \tag{4}$$

Where; $m$ = blowing ratio

| | | | |
|---|---|---|---|
| $\rho_c$ = coolant density | ($kg.m^{-3}$) | $\rho$ = mainstream density | ($kg.m^{-3}$) |
| $v_c$ = coolant velocity | ($m.s^{-1}$) | $v$ = mainstream velocity | ($m.s^{-1}$) |

Mainstream and coolant velocity were varied using their respective fan controller to get the necessary blowing ratio. Ambient air was used in both experiments to simulate the mainstream hot flow and coolant flow.

## RESULTS AND DISCUSSIONS

### Flat Plate Test

Experiments were conducted only at the upper surface of the test plate that was already coated with TLC. The duration for the experiment was 90 seconds for the validation of the one dimensional semi infinite solid heat transfer assumption. Figure 4 below shows the temperature distribution of the flat plate and also the voltage rise of the L.E.D. during the experiment.

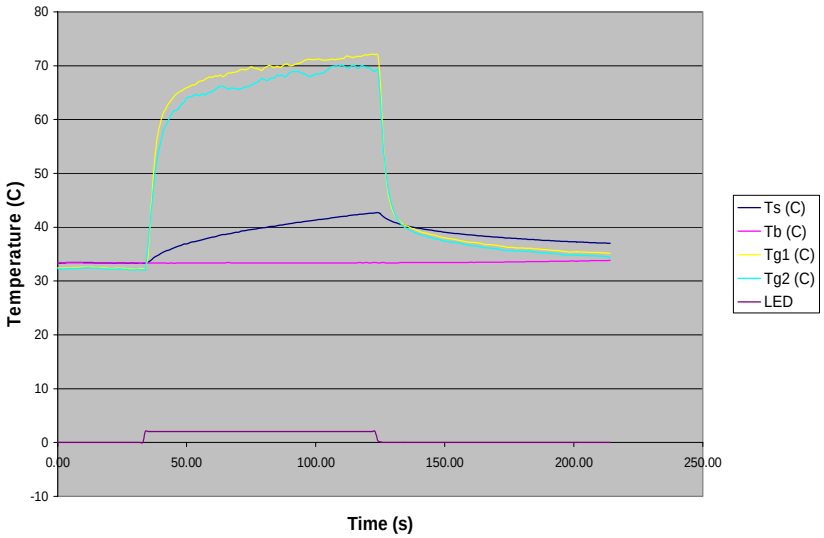


*Figure 4: Temperature history for flat plate test*

The data measured were gathered only in the 90 seconds immediately after the L.E.D on as indicated by the voltage rise (violet line) at the bottom of the figure. The blue line in Figure 4 indicates the surface temperature ($T_s$) of the test plate coated with liquid crystals. The pink line indicates the back temperature ($T_b$) of the test plate. This line is used to monitor the back temperature to ensure that the experiment is performed with heat flow is not completely penetrates the test plate. The yellow line ($T_{g1}$) and green line ($T_{g2}$) indicates the gas temperature for the mainstream flow.

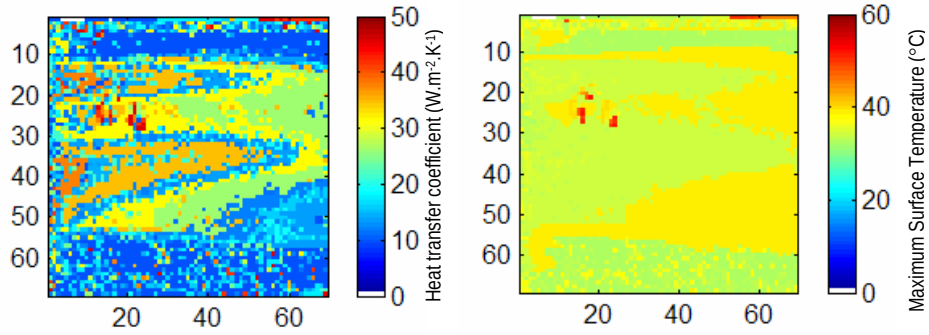


*Figure 5: Heat transfer coefficient and maximum surface temperature distribution on the flat plate*

Figure 5 illustrates the maximum surface temperature and heat transfer coefficient distribution on the test plate after 90 seconds. The images captured from the digital camcoder were processed using Matlab routine similar to the approach reported by Abu Talib [13]. Briefly, the maximum surface temperature and the heat transfer coefficients distribution for the test plate were unevenly distributed. This was caused by the non-uniformity of the flow at the exit of the mainstream duct. Further improvements on the mainstream duct design could be done to eliminate this effect.

Abu Talib et al. [14] reported the maximum percentage error for one-temperature step problem was 27.9 %. Hence, the heat transfer coefficients found from the experiment were in the range of 25-35 ± 7 $W.m^{-2}.K^{-1}$. The standard correlation used for this experiment was an expression for fully developed turbulent flow in smooth tubes, recommended by Dittus and Boelter [15].

The Dittus and Boelter correlation is as follows:

$$Nu = 0.023\ Re^{0.8}\ Pr^{n}\ ; \quad (5)$$

where $n = 0.3$ (for cooling of the fluid) and Nu is the Nusselt number.

The above equation is valid only for fluids with Prandtl numbers ranging from 0.6 to 100 and with Reynolds number ranging from 2500 to 125000. The Reynolds number was based on the hydraulic diameter of the test section. From the tests conducted, the Prandtl number of air is 0.71, and a Reynolds number of 33391 which satisfied the requirements for using the Dittus and Boelter correlation. The heat transfer coefficients gathered from eauation (5) was ranging from 25.7-27.6 $W.m^{-2}.K^{-1}$. The local heat transfer coefficients gathered from the tests were found to falls into the range of the standard correlation of heat transfer coefficient. Hence the data obtained from the test can be considered reliable and the same strategy was used on the film cooling test.

**Film Cooling Test**

Experiments were conducted only at the upper surface of the test plate that was already coated with TLC for 90 seconds. Tests were conducted to evaluate the film cooling effectiveness for different blowing ratios. The blowing ratio chosen were 0.94, 0.83, 0.64, and 0.50. Frames used in this section were taken at the time of the L.E.D. off. The reason by choosing these frames was because to get the most colour play of the liquid crystal. In these experiments which dealt with cooling holes, the places of interest were only at the downstream of the film cooling hole.

***Blowing Ratio 0.94***

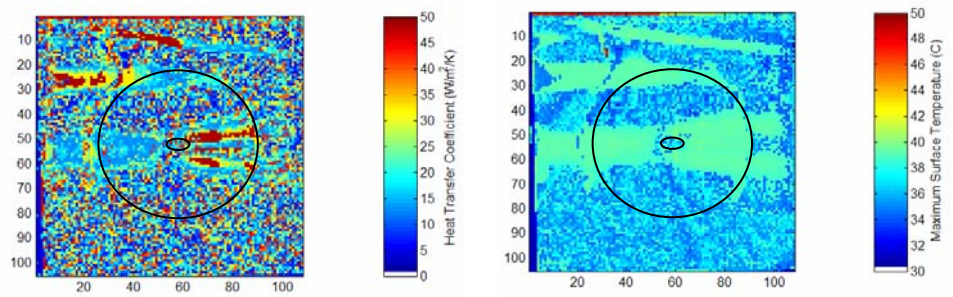


*Figure 6: Heat transfer coefficient, and the maximum surface temperature for blowing ratio of 0.94*

Figure 6 illustrates the whole field distribution of the local heat transfer coefficient and maximum surface temperature for blowing ratio of 0.94. The black circle in the figure indicates the removable part of the test plate. The small black elliptical shape in the figure indicates the cooling hole at the test plate. From the figure, there were almost no cooling processes downstream of the cooling hole. As expected, the high heat transfer coefficients can be observed on the surface for this particular blowing ratio.

***Blowing Ratio 0.83***

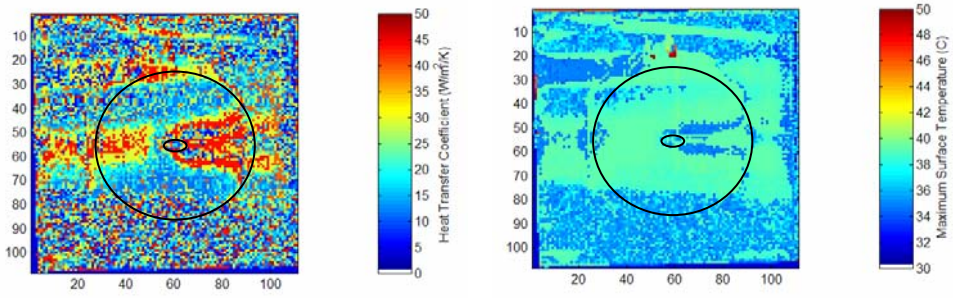


*Figure 7: Heat transfer coefficient and maximum surface temperature for blowing ratio of 0.83*

Referring to Figure 7, it illustrates the heat transfer coefficient and maximum surface temperature distribution for blowing ratio of 0.83. There were slight improvements in the cooling process downstream of the cooling hole. Overall, the heat transfer coefficients were still high during the experiment for this particular blowing ratio. Due to some cooling activities, the results for the maximum surface temperature and heat transfer coefficients for this particular blowing ratio were quite low than the blowing ratio of 0.94.

***Blowing Ratio 0.64***

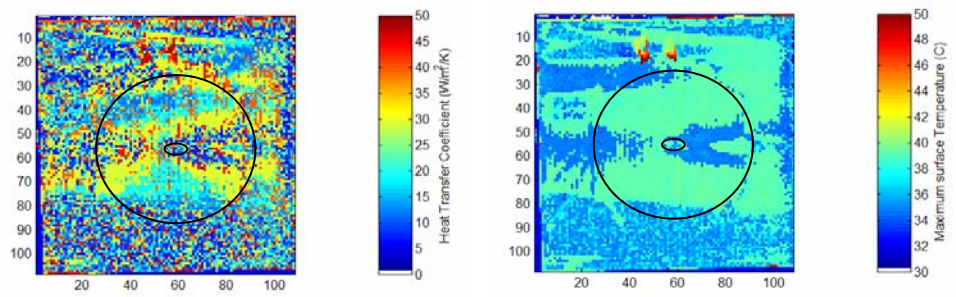


*Figure 8 Heat transfer coefficient and maximum surface temperature for blowing ratio of 0.64*

Figure 8 illustrates the heat transfer coefficient and maximum surface temperature distribution for blowing ratio of 0.64. From the figure, it could be seen clearly that there were an obvious improvement downstream of the film cooling hole. Overall, the heat transfer coefficients were low during the experiment for this particular blowing ratio, and downstream of the cooling hole, there were a few places with very low heat transfer coefficients due to the cooling processes. The values of the normalized temperature were low for this experiment. Due to better cooling activities, the results for the maximum surface temperature and heat transfer coefficients for this particular blowing ratio were lower than the blowing ratios of 0.94 and 0.83.

***Blowing Ratio 0.50***

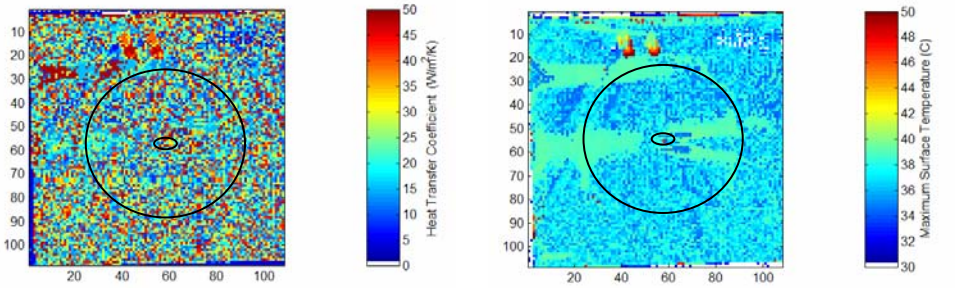


*Figure 9: Heat transfer coefficient and maximum surface temperature for blowing ratio of 0.50*

Figure 9 shows the heat transfer coefficient and maximum surface temperature distribution for blowing ratio of 0.50. From the figure, effectiveness of the film cooling is reduced in the region downstream of the cooling hole. Overall, the heat transfer coefficients, and the values for maximum surface temperature found were moderate during the experiment for this particular blowing ratio.

From the results gathered for all blowing ratios, the highest film cooling effectiveness could be seen at blowing ratio 0.64, followed by blowing ratio 0.50, blowing ratio 0.83 and the least film cooling effectiveness was at blowing ratio 0.94. When comparing results for blowing ratio 0.50 and 0.83, it was found that there were higher heat transfer coefficients downstream of the cooling hole for blowing ratio 0.83 than the blowing ratio for 0.50.

Even though film cooling generated at blowing ratio 0.50 was not as much as in blowing ratio 0.83, the cooling effectiveness was higher for blowing ratio at 0.50 than the blowing ratio at 0.83. This result agreed with Nasir et al. [2] and Dittmar et al. [1] which stated that higher film cooling efficiencies could be found at lower blowing ratios within the range of 0.5 to 0.7. At higher blowing ratios, which means that the coolant flow velocity is almost the same as the mainstream velocity, the film cooling structure will dissipate just downstream of the cooling hole due to the velocity of the mainstream flow which is nearly the same as the coolant flow velocity. Therefore, there is a need in maintaining higher mainstream velocity to ensure that the cooling jets will remain downstream of the cooling holes and reducing the possibilities of cooling jet lift-off. Cooling jet lift-off means that the coolant flow does not remain intact when the flow was ejected from the cooling hole.

Illustrations of the film cooling for all blowing ratios are shown in Figure 10. For blowing ratio of 0.94 and blowing ratio of 0.83, ejected film cooling flow penetrated through the mainstream. Only a fraction of the film cooling structure provides a protective layer to the surface. For blowing ratio of 0.50, the jet flow is effectively developed into a film cooling flow. Eventually it provides better film cooling protection than for blowing ratio at 0.94 and 0.83 because the film cooling generated was near to the surface and it provides better protective layer to the surface. For blowing ratio of 0.64, the film cooling structure generated at this blowing ratio was

neither lifted too far above the surface nor too low near the surface. Therefore, it could provide the ideal and widest range of protective layer to the surface area of the plate. It can be proposed that the best film cooling effectiveness was found at this particular blowing ratio, $m = 0.64$.

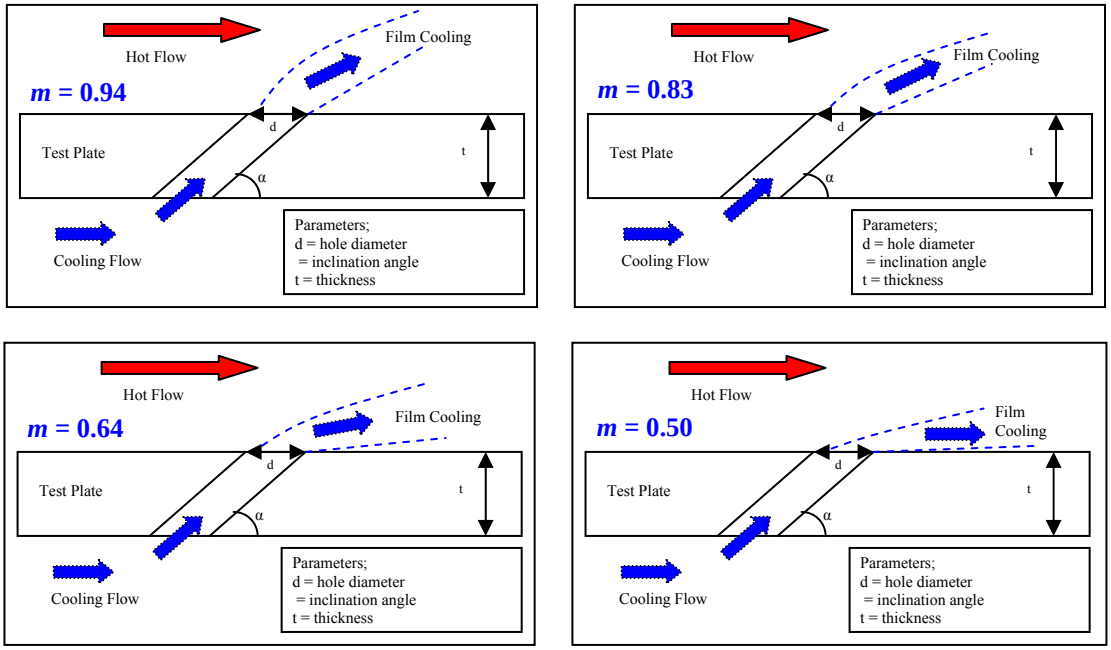


*Figure 10: Film cooling representation at blowing ratio of 0.94, 0.83, 0.64 and 0.50*

## CONCLUSIONS

For the flat surface film cooling experiments, the blowing ratio of 0.64 and 0.50 shows good film cooling effectiveness than of the blowing ratio of 0.94 and 0.83. This result indicates a good agreement with the literatures review made earlier which stated that better film cooling effectiveness could be found at lower blowing ratio. The measurement technique using thermochromic liquid crystal (TLC) technique was proven accurate and reliable to measure the complete distribution of heat transfer coefficient and maximum surface temperature distributions.

## ACKNOWLEDGEMENT

The authors would like to thank Mr A.H Ariffin for fabricating the test plates. Special thanks to Universiti Putra Malaysia for the financial support.

## REFERENCES

[1] Dittmar, J., Schulz, A., and Wittig, S. (2004) Adiabatic effectiveness and heat transfer coefficient of shaped film cooling holes on a scaled guide vane pressure side model. International Journal of Rotating Machinery, **10**(5): 345-354.

[2] Nasir, H., Ekkad, S.V., and Acharya, S. (2001) Effect of compound angle injection on flat surface film cooling with large streamwise injection angle. Experimental Thermal and Fluid Science, **25**: 23-29.

[3] Yuen, C.H.N and Martinez-Botas, R.F. (2003) Film cooling characteristic of a single round hole at various angles in a crossflow: Part I – Effectiveness. International Journal of Heat Mass Transfer, **46**: 221-235.

[4] Yuen, C.H.N and Martinez-Botas, R.F. (2003) Film cooling characteristic of a single round hole at various angles in a crossflow: Part II - Heat Transfer Coefficient. International Journal of Heat Mass Transfer, **46**: 237-249.

[5] Drost, U., Bölcs, A., and Hoffs, A. (1997) Utilization of the transient liquid crystal technique for film cooling effectiveness and heat transfer investigations on a flat plate and a turbine airfoil. 97-GT-26.

[6] Mayhew, J.E., Baughn, J.W., and Breyley, A.R. (2003). The effect of freestream turbulence on film cooling adiabatic effectiveness. International Journal of Heat and Fluid Flow, **24**: 669-679.
[7] Lee, J.S., and Jung, I.S. (2002) Effect of bulk flow pulsations on film cooling with compound angle holes. International Journal of Heat Mass Transfer, **45**: 113-123.
[8] Garg, V.K., and Gaugler, R.E., (1997), Effect of coolant temperature and mass flow on film cooling of turbine blades, International Journal of Heat Mass Transfer, **4**(2): 435-445.
[9] Jaafar, A.A, Abu Talib, A.R., Mokhtar, A.S., Abd.Rahim, I., Arora, P.R and Megat Ahmad, M.M.H (2005) Combined Experimental and Numerical Investigation on a Film Cooling Flow over a Flat Surface. Proceedings, National Conference on Advances in Mechanical Engineering, Kuala Lumpur.
[10] Mohd Saiah, H.R (2006) Heat transfer measurements on flat plate surface film cooling. Final Year Project Report, Department of Aerospace Engineering, UPM, Malaysia.
[11] Ekkad, S.V., and Han, J.C. (2000) A transient liquid crystal thermography technique for gas turbine heat transfer measurements. Measurement Science Technology, **11**: 957-968.
[12] Schultz, D.L and Jones, T.V (1973) Heat transfer measurements in short duration hypersonic facilities. AGARD-AG-165.
[13] Abu Talib, A.R (2003) Detailed investigation of the low-temperature analogy of an aircraft engine standard fire-test. D.Phil Thesis, Department of Engineering Science, University of Oxford, U.K.
[14] Abu Talib, A.R., Neely, A.J., Ireland, P.T and Mullender, A.J (2004) A novel liquid crystal image processing technique using multiple gas temperature steps to determine heat transfer coefficient distribution and adiabatic wall temperature. Journal of Turbomachinery, **126**(4): 587-596.
[15] Dittus, F.W and Boelter, L.M.K (1930) University of California (Berkeley) Pub. Eng., 2: 443.

## NOMENCLATURE

| | | |
|---|---|---|
| $c_p$ | specific heat of test surface | ($J.kg^{-1}.K^{-1}$) |
| $d$ | diameter/hydraulic diameter | (m) |
| $h$ | heat transfer coefficient | ($W.m^{-2}.K^{-1}$) |
| $k$ | thermal conductivity | ($W.m^{-1}.K^{-1}$) |
| $L$ | characteristic length | (m) |
| M | mach number | |
| Nu | Nusselt number, $\mathrm{Nu} = \frac{hL}{k}$ | |
| Pr | Prandtl number, $\mathrm{Pr} = \frac{\mu_\infty c_p}{k}$ | |
| Re | Reynolds number, $\mathrm{Re} = \frac{\rho_\infty v_\infty d}{\mu_\infty}$ | |
| $T$ | temperature | (°C) |
| $t$ | time of colour change to prescribed colour | (s) |
| t | thickness | (m) |
| $v$ | velocity | ($m.s^{-1}$) |

*Greek*

| | | |
|---|---|---|
| $\alpha$ | thermal diffusivity of test surface | ($m^2.s^{-1}$) |
| $\eta$ | film cooling effectiveness | |
| $\mu$ | dynamic viscosity | ($kg.m^{-2}.s^{-1}$) |
| $\rho$ | density | ($kg.m^{-3}$) |

*Subcripts*

| | |
|---|---|
| $\infty$ | freestream |
| $c$ | coolant |
| $f$ | film |
| $i$ | initial |
| $m$ | mainstream |
| $w$ | wall |